Physics Letters B 833 (2022) 137309

Contents lists available at ScienceDirect

Physics Letters B

www.elsevier.com/locate/physletb

Mass measurements towards doubly magic ^{78}Ni: Hydrodynamics versus nuclear mass contribution in core-collapse supernovae

S. Giraud [a,b,*], L. Canete [c,d], B. Bastin [a], A. Kankainen [c], A.F. Fantina [a], F. Gulminelli [e], P. Ascher [f], T. Eronen [c], V. Girard-Alcindor [a,j,k], A. Jokinen [c], A. Khanam [g,h,c], I.D. Moore [c], D.A. Nesterenko [c], F. de Oliveira Santos [a], H. Penttilä [c], C. Petrone [i], I. Pohjalainen [c], A. De Roubin [c], V.A. Rubchenya [c,1], M. Vilen [c,l], J. Äystö [c]

[a] GANIL, Bd Henri Becquerel, BP 55027, F-14076 Caen Cedex 5, France
[b] National Superconducting Cyclotron Laboratory, Michigan State University, East Lansing, MI 48824, USA
[c] University of Jyvaskyla, P.O. Box 35, FI-40014 University of Jyvaskyla, Finland
[d] University of Surrey, Guildford, GU2 7XH, United Kingdom
[e] LPC (CNRS/ENSICAEN/Université de Caen Normandie), UMR6534, 14050 Caen Cedex, France
[f] CENBG, CNRS/IN2P3—Université Bordeaux 1, 33175 Gradignan Cedex, France
[g] Department of Applied Physics, Aalto University, P.O. Box 15100, FI-00076 Aalto, Finland
[h] Department of Physics, University of Helsinki, P.O. Box 43, FI-00014 Helsinki, Finland
[i] IFIN-HH, P.O. Box MG-6, 077125 Bucharest-Magurele, Romania
[j] Université Paris-Saclay, CNRS/IN2P3, IJCLab, 91405 Orsay, France
[k] TU Darmstadt, Schlossgartenstraße 9, D-64289 Darmstadt, Germany
[l] Experimental Physics Department, CERN, CH-1211 Geneva 23, Switzerland

ARTICLE INFO

Article history:
Received 27 January 2022
Received in revised form 6 June 2022
Accepted 12 July 2022
Available online 16 July 2022
Editor: D.F. Geesaman

Keywords:
Nuclear mass
Penning trap
Shell gap
Core-collapse supernova

ABSTRACT

We report the first high-precision mass measurements of the neutron-rich nuclei ^{74,75}Ni and the clearly identified ground state of ^{76}Cu, along with a more precise mass-excess value of ^{78}Cu, performed with the double Penning trap JYFLTRAP at the Ion Guide Isotope Separator On-Line (IGISOL) facility. These new results lead to a quantitative estimation of the quenching for the $N = 50$ neutron shell gap. The impact of this shell quenching on core-collapse supernova dynamics is specifically tested using a dedicated statistical equilibrium approach that allows a variation of the mass model independent of the other microphysical inputs. We conclude that the impact of nuclear masses is strong when implemented using a fixed trajectory as in the previous studies, but the effect is substantially reduced when implemented self-consistently in the simulation.

Core-collapse supernovae (CCSN) represent the end point of stellar evolution for stars with masses greater than about 8-10 solar masses. Despite the enormous progress made in CCSN simulations in the last decades, several aspects still deserve clarification [1]. While many studies show the importance of the microphysics on the collapse dynamics (see, e.g. [1–3] for a review), the precise role of each microphysics input has not been fully pinpointed. This is because, due to the coupling of the microphysics with the hydrodynamics, quantifying the specific impact of each nuclear input is not trivial. However, the CCSN simulations of ref. [4] have shown that the uncertainties on the electron-capture rates on individual nuclei during infall induce stronger modifications on the mass of the inner core at bounce and the maximum of the neutrino luminosity peak than the other uncertainties of the collapse phase, namely the progenitor model, the equation of state, or the neutrino treatment. Those electron-capture rates depend on the nuclear structure details of the relevant nuclei which are still experimentally unconstrained, but a basic ingredient is given by the electron-capture Q-value, Q_{EC}, which is solely determined by the nuclear masses. Previous studies [5,6] have shown that the impact of the neutron shell-gap strengths on the matter composition relevant for CCSN could change the overall electron-capture rates up to $20 - 40\%$. In particular, masses of nuclei around the double-

* Corresponding author at: National Superconducting Cyclotron Laboratory, Michigan State University, East Lansing, MI 48824, USA.
E-mail addresses: giraud@frib.msu.edu (S. Giraud), l.canete@surrey.ac.uk (L. Canete).
[1] Deceased.

https://doi.org/10.1016/j.physletb.2022.137309

shell closures with magic neutron N and proton numbers Z at ($N = 50, Z = 28$) and ($N = 82, Z = 50$), have been shown to be especially relevant both in CCSN and r-process calculations [5,7–15], thus highlighting the need for new experimental data in those regions of the nuclear chart. The β-decay lifetime measurements of ^{78}Ni at NSCL [16] and at RIBF [17], the recent precise mass measurements of $^{77-79}$Cu using the ISOLTRAP Penning trap at CERN [18] and the identification of the first 2^+ state of ^{78}Ni at a rather large excitation energy at RIBF [19], suggest a weak quenching for the $N = 50$ shell gap at around $Z = 28$. However, due to the scarce experimental information in this exotic part of the Nuclide Chart, questions remain still open regarding the evolution of the $N = 50$ shell gap; the most important one being: to what extent is this shell closure preserved in case of the doubly magic nucleus ^{78}Ni?

In addition to the excitation energy of the first 2^+ states and their corresponding reduced transition probabilities, another relevant parameter for this question is the evolution of the empirical two-neutron shell-gap energies Δ_{2n} for different isotonic chains. In this Letter we report relevant new mass measurements along the nickel, copper and zinc isotopes. We present the first precise mass measurements of ^{74,75}Ni, extending the previous set of measurements done at the JYFLTRAP Penning trap for the nickel isotopes in [20]. New mass measurements of ^{76,77,78}Cu and ^{79}Zn isotopes, were also performed with the purpose of improving the mass precision. These newly measured values are then used to study systematics of the experimental Δ_{2n} and are compared with the predictions of several theoretical mass models. Finally, using a dedicated extended nuclear statistical equilibrium formalism [10], incorporating a full nuclear distribution in the equation of state in a CCSN simulation, we have consistently studied the effect of the shell-gap quenching on the electron-capture rates in the core-collapse dynamics.

The mass measurements were carried out at the Ion-Guide Isotope Separator On-Line (IGISOL) facility in Jyväskylä [21], Finland. The studied neutron-rich isotopes were produced by induced fission, using a 35 MeV, 10 μA proton beam impinging on a 15 mg cm^{-2}-thick natural uranium target. The fission fragments were thermalized in a helium buffer gas and extracted from the gas cell dominantly in a singly-charged state. Following transport through a radio-frequency sextupole ion guide [22], the ions were accelerated to 30 keV and mass separated passing through a magnetic dipole with a mass resolving power of $m/\Delta m \approx 500$. The continuous beam was cooled and bunched in a radio-frequency quadrupole (RFQ) cooler buncher [23] prior to injection into the double Penning trap mass spectrometer JYFLTRAP [24]. The first trap was used for isobaric purification using the buffer-gas cooling technique [25]. The precision mass measurements were carried out in the second trap employing the time-of-flight ion-cyclotron-resonance (TOF-ICR) technique [26]. The ion's cyclotron resonance frequency $\nu_c = qB/(2\pi m)$, where q and m are the charge and the mass of the ion, and B the magnetic field strength, is determined by applying a quadrupolar excitation with a frequency ν_{rf} near the expected cyclotron frequency ν_c. When $\nu_{rf} = \nu_c$, the ions extracted from the trap have the shortest flight time to a micro-channel plate detector. A typical TOF-ICR resonance spectrum for ^{75}Ni$^+$ is presented in Fig. 1. A 200-ms quadrupolar excitation scheme was applied for ^{74}Ni and ^{79}Zn, 100-ms for ^{75}Ni and ^{77}Cu, and 1120-ms for ^{76}Cu. Ramsey's method of time-separated oscillatory fields [27,28] with an excitation pattern of 25-50-25 ms (On-Off-On) was used for ^{78}Cu. Cyclotron frequency measurements of the ions of interest were alternated with measurements of a stable reference ion with a well-known mass to determine the magnetic field strength at the time of the actual measurement. The cyclotron frequency ratio r between the studied singly-charged reference ions ($\nu_{c,ref}$) and the ions of interest (ν_c), $r = \nu_{c,ref}/\nu_c$, was

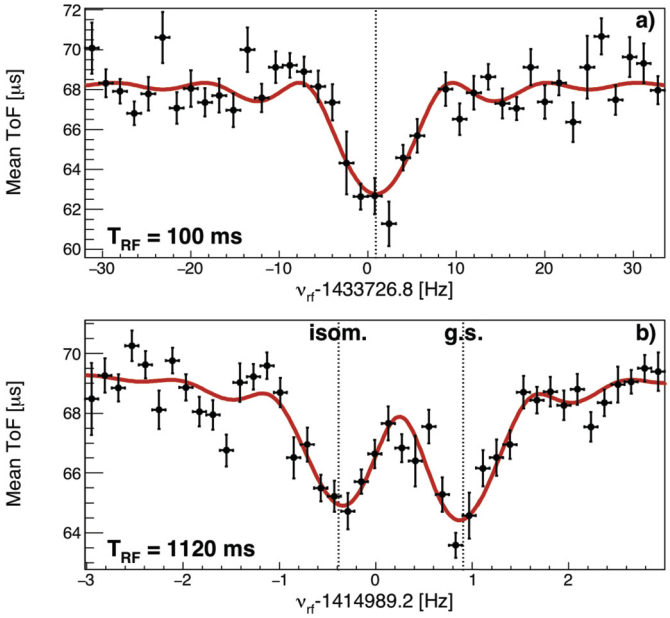

Fig. 1. TOF-ICR spectra for ^{75}Ni$^+$ (a) and ^{76}Cu$^+$ (b) collected with 100-ms and 1120-ms excitation times T_{RF}, respectively. The solid red line is a fit of the theoretical line shape [26] to the data (black points) with corresponding error bars. Vertical dashed lines indicate the positions of the resonance frequencies.

employed to deduce the mass of the nuclide of interest using the equation: $m = r(m_{ref} - m_e) + m_e$, where m, m_{ref} and m_e, are the atomic mass of the nuclide of interest, the reference nuclide ^{84}Kr ($m = 83.911497727(4)$ u [29] and the mass of the electron [29], respectively. It should be noted that electron binding energies for valence electrons are much smaller than statistical uncertainties and were negligible in the latter equation. The final frequency ratios and mass values were calculated as weighted means over typically 3–5 measurements. Systematic uncertainties related to the magnetic field fluctuations ($8.18 \times 10^{-12} \times \Delta t$ min^{-1} [30], where Δt represents the time between two reference measurements) and mass-dependent uncertainties ($2.2 \times 10^{-10} \times (m - m_{ref})/$ u [31]) were quadratically added to the statistical uncertainties of the frequency ratios ($\sim 2 - 20 \times 10^{-8}$).

The measured frequency ratios and the corresponding mass-excess (ME) values are summarized in Table 1. The mass values of ^{74,75}Ni have been determined precisely for the first time. Our experimental values are somehow higher than the extrapolations of the Atomic Mass Evaluation 2020 (AME2020) [29]: differences of 249(200) keV (^{74}Ni) and 184(201) keV (^{75}Ni). In fact, Ref. [32] reports on the mass of ^{74}Ni but this has not been considered in AME2020 due to the large error bar. Our measured value, which is 759(990) keV higher than the value in [32], provides a good reference point for the expected future measurements of more exotic species in this region via other methods, such as storage rings [33,34], Multi-Reflection Time-of-Flight Mass Spectrometry (MR-TOF-MS) [35,36] or $B\rho$-ToF [37,38]. Moreover, the new mass values of ^{74,75}Ni will improve the extrapolations toward ^{78}Ni in the forthcoming mass evaluations. Regarding ^{76}Cu, the two long-living states were resolved in the TOF-ICR spectra (see Fig. 1) and measured accordingly. In addition, we used the phase-imaging ion cyclotron resonance technique [39] to further identify the states based on their half-lives and to confirm their energy difference. The relatively large difference to the ISOLTRAP measurements [18,40] can be explained if mixtures of both states have been measured due to a lower resolution of the TOF-ICR technique in their work. Nevertheless, the new mass values of ^{77,78}Cu are in good agreement with the recent ISOLTRAP Penning trap and multi-reflection time-of-flight mass spectrometer mea-

Table 1
List of nuclei and their properties (half-life $T_{1/2}$, spin-parity I^{π} based on Ref. [29]), as well as the measured frequency ratios $r = \nu_{ref}/\nu$ and mass-excess values "ME" for the ground states from this work in comparison with the literature values from the AME2020 [29]. '#' denotes a value based on extrapolations. The difference between the two mass-excess values (Diff. = ME_{lit}-ME_{JYFL}) is also indicated. Singly-charged ions of ^{84}Kr (m = 83.911497727(4) u [29]) were used as a reference for all studied cases.

Nuclide	$T_{1/2}$(ms)	I^{π}	r	ME_{JYFL} (keV)	ME_{lit} (keV)	Diff. (keV)
^{74}Ni	507.7 (4.6)	0^+	0.881260877(44)	-48451.4 (3.5)	-48700 (200)#	-249 (200)
^{75}Ni	331.6 (3.2)	$9/2^+$#	0.893234508(187)	-44055.9 (14.7)	-44240 (200)#	-184 (201)
^{76}Cu	637.7 (5.5)[a]	3^-[a]	0.905062917(26)	-51011.4 (2.0)	-50981.6 (0.9)	29.8 (2.2)
^{77}Cu	470.3 (1.7)	$5/2^-$	0.917007818(60)	-48861.5 (4.7)	-48862.8 (1.2)	-1.3 (4.9)
^{78}Cu	330.7 (2.0)	(6^-)	0.928977359(96)	-44785.7 (7.5)	-44789 (13)	-3.3 (15.0)
^{79}Zn	746 (42)	$9/2^+$	0.940784139(40)	-53431.8 (3.1)	-53432.3 (2.2)	-0.5 (3.8)

[a] The validity of these two properties will be discussed in a separate paper.

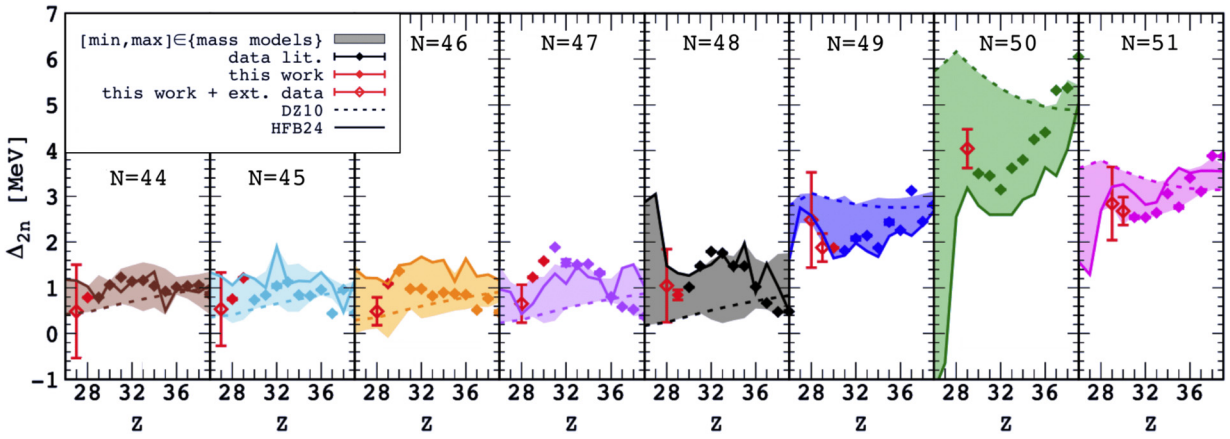

Fig. 2. Empirical two-neutron shell-gap energies Δ_{2n} for different isotonic chains N=46-52 as function of Z. The red points represent the gap obtained using one or several of our measured mass-excess values (empty red point if extrapolated mass from [29] is used). The colored (except red) points are the gap obtained using experimental values from [29]. The shaded areas represent the range of mass models (DZ10 [45], DZ28 [45], FRDM12 [46], HFB-24 [47], WS4 [48], KTUY05 [49]). The dashed (solid) line shows the predictions of the DZ10 (HFB-24) model.

surements [18]. The precision for ^{78}Cu has been improved thanks to the Ramsey's method. Furthermore, the measured ground-state mass-excess value of ^{79}Zn agrees with the values reported from ISOLTRAP, -53435.1(3.9) keV [41] and JYFLTRAP, -53430.9(2.7) keV [42]. We have also determined the mass for the $1/2^+$ isomeric state ^{79m}Zn. Our results on the isomers will be discussed in a separate paper. The recently published [43] ground-state mass values of ^{67}Fe and ^{69,70}Co obtained during the same experiment are also taken into account in the following analysis.

The new mass-excess values (see Table 1) were employed to investigate the evolution of the empirical two-neutron shell-gap energies $\Delta_{2n}(N,Z) = ME(N+2,Z)+ME(N-2,Z)-2ME(N,Z)$ toward $N = 50$ and $Z = 28$. For $Z = 28$ and for $N = 44-49$, the Δ_{2n} from the AME2020 [29] mass-excess values are significantly different from the Δ_{2n} obtained with our measurements (in average 288 keV absolute difference): from -184 keV to +497 keV. In Fig. 2, eight new Δ_{2n} values are presented and ten more obtained including extrapolated mass values from AME2020, thus extending the experimental $\Delta_{2n}(N,Z)$ trends far from stability. For the magic neutron number $N = 50$, the empirical two-neutron shell-gap energy is between ~3-6 MeV for $Z = 29-40$, much higher than for the neighboring isotonic chains. The $N = 50$ empirical shell gap is weakly reinforced as $Z = 28$ is approached, in agreement with the recently observed doubly magic behavior of ^{78}Ni [18,19]. The empirical two-neutron shell-gap energies were compared to the predictions of several theoretical mass models conventionally used in astrophysical studies. The colored bands shown in Fig. 2 represent the range of shell-gap energies covered by the studied mass models. For comparison, we have indicated with solid and dashed lines the gaps predicted by the HFB-24 and DZ10 mass models, previously used in [4,8] to assess the influence of nuclear masses on the core collapse. Among the different mass models, HFB-24 is the only one coming from a microscopic energy density functional [44], which explains the complex non-smooth behavior shown in Fig. 2. It predicts a strong quenching for the $N = 50$ gap, extending up to ^{78}Ni. In the region close to $Z = 28$, the DZ10 mass model overestimates the neutron shell-gap energies for and above N=49 and underestimates them below N=49. The opposite behavior is observed for HFB-24. The strong shell gap predicted by the DZ10 model for $N = 50$ explains why nuclear statistical distributions are more peaked and persist around magic nuclei with respect to those predicted by HFB-24 for which the $N = 50$ closure is weaker. In addition, the trends of the empirical two-neutron shell-gap energies, especially for $N = 50$, are better reproduced by the HFB-24 mass model than DZ10. Interestingly, the shell-gap quenching observed for $N = 50$ - in good agreement with the predictions of the microscopic HFB-24 model - appears strongly reduced in ^{78}Ni, even if extrapolated values leading to non-negligible error bars are needed. We observe that the HFB-24 and DZ10 mass models differ considerably in the Δ_{2n} predictions: for $N = 50, Z = 28$, the discrepancy amounts to 3.6 MeV. Therefore, the use of these two distinct mass models can address the question of the mass-model dependence in astrophysical scenarios like CCSN modeling. Note that results from another mass model (e.g. FRDM12 [46]) would thus lead to an intermediate conclusion.

Previous CCSN studies [5,6] have been performed considering typical (fixed) collapse trajectories, i.e. a predetermined set of densities (ρ), temperatures (T), and electron fractions (Y_e). Here, we

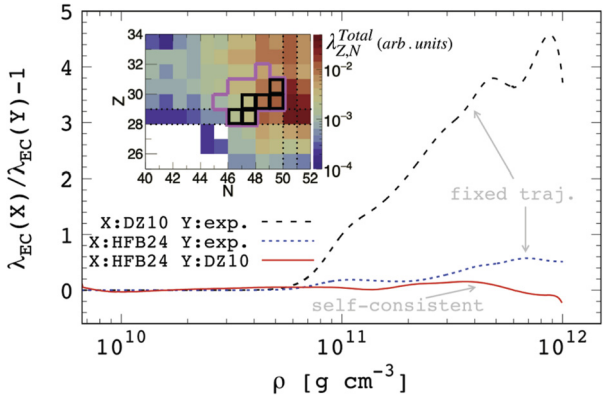

Fig. 3. Relative difference between the total electron-capture rate obtained using the distribution of the HFB-24 mass model compared to DZ10 as function of baryonic density obtained for a self-consistent (solid line) trajectory. The inset is adapted from [4], showing the most relevant nuclei for electron captures up to neutrino trapping using HFB-24 mass model and the self-consistent trajectory method. The black squares indicate the nuclei with our new mass results. The pink contour shows the nuclei for which the Q_{EC} precision is improved thanks to our work. Their impact is well illustrated by the partial relative difference between the rates obtained with the two reference mass models and our experimental values for a fixed trajectory (dashed and dotted lines). See text for details.

perform CCSN numerical simulation using the ACCEPT code (see [4,50–52] for details). The latter is a spherically symmetric core-collapse code solving general relativistic hydrodynamics, with neutrinos treated in a simple leakage-type multi-group scheme (here, the trapping density has been fixed to 10^{12} g cm^{-3}). In order to assess the mass-model dependence, we use the perturbative method developed in [8] built upon the Lattimer & Swesty [53] equation of state, employing the DZ10 and HFB-24 mass models. Electron-capture rates are computed with the parametrization from [54]. Results are shown in Fig. 3, where the relative difference between the instantaneous electron-capture rates calculated with the DZ10 and HFB-24 mass models are plotted as a function of baryonic density during the collapse, using a self-consistent trajectory (solid line). Since DZ10 (HFB-24) does not allow (allows) for shell-gap quenching, the ordinate in Fig. 3 can be considered as a quantitative prediction of the impact of the quenching on the rates. To evaluate the impact of the newly measured masses, we have also calculated the partial relative difference between the sums of the rates of the nuclei in the pink contour Fig. 3, obtained with either the DZ10 (dashed line) or HFB-24 (dotted line) mass models and our new experimental masses, using a fixed trajectory. All the curves are very similar for $\rho \lesssim 5\times10^{10}$ g cm^{-3}, since nuclei are located around $A\sim60$ ($Z\sim28$) where the shell gaps at $Z=28$, $N=32$ from DZ10 (1.79 MeV) and HFB-24 (1.49 MeV) models are not dramatically different. Therefore, the relative electron-capture rates differ less than 10% in this phase. In subsequent stages of the collapse, discrepancies arise, because the populated nuclei are located near, between, or even beyond the doubly magic nuclei ^{78}Ni and ^{132}Sn, for which the DZ10 and HFB-24 predictions differ. Comparing the dashed and dotted lines, we can notice that the rates obtained with HFB-24 show a much closer agreement with those calculated using the new experimental mass values, confirming that this model gives an adequate description of the masses (see Fig. 2), and has therefore to be preferred for nuclei without experimentally determined mass values. Conversely, if DZ10 is used, the rates can be overestimated up to a factor of 5. This clearly shows the importance of the newly measured mass values to assess the reliability of the theoretical models for astrophysical applications. The difference between the two models can be qualitatively understood from the fact that a strong $N=50$ gap around ^{78}Ni, such as in DZ10, disfavors a strong neutronization, thus leading to an overestimation of the production of nuclei with relatively high Q_{EC} values. Such a strong $N=50$ gap is excluded by our mass measurements. Our results for the fixed trajectory are qualitatively in good agreement with Refs. [5,6], suggesting a strong impact of the used mass model on the electron-capture rates. Surprisingly, this effect is reduced when a self-consistent treatment is done; indeed, the feedback effect is sufficiently strong to almost completely erase the effect of the mass model. Indeed, even if the HFB-24 mass model is still more efficient in neutronizing the medium during most of the time of the self-consistent trajectory (85 % of the neutronization process), in the last stage ($> 6\times10^{11}$ g cm^{-3}) when the total electron-capture rate is higher, the DZ10 electron-capture rate overcomes the HFB-24 rate during a short period (0.6 % of the neutronization process). It turns out that this is long enough to compensate the integrated effect of the HFB-24 mass model on the electron fraction at the neutrino trapping density, thus inducing only small differences on the CCSN properties at bounce. However, we have to underline that for a final word to be said, the individual electron-capture rates should be experimentally constrained. This requires, in addition to the masses (Q_{EC} values), a new generation of Total Absorption Spectrometers and the use of charge-exchange reactions setups with radioactive beams [55].

Ideally, experimentally measured mass values instead of theoretical mass models would be used for all relevant nuclei. The precision mass measurements of this work provide more precise Q_{EC} values for around 12 key nuclei contributing the most to the total electron-capture rate during the core collapse (see the inset of Fig. 3). This is an important first step to provide accurate electron-capture rate calculations for CCSN simulations, however, more experiments are needed to fully base the simulations on experimental values.

In conclusion, using the JYFLTRAP double Penning trap the masses of the neutron-rich magic nuclei ^{74,75}Ni and the ground state of ^{76}Cu were precisely measured for the first time. In addition, we presented new mass measurements of ^{77,78}Cu and ^{79}Zn. The empirical two-neutron shell gaps obtained with our data suggest the preservation of the doubly magic nature of ^{78}Ni in agreement with the recent results obtained in [18,19]. These results will provide key reference points for expected future measurements of more exotic species in this region via new experimental methods [33–38], and allow more precise theoretical predictions e.g. for nuclear interactions in this region. Finally, it will impact AME predictions. By comparing the updated empirical two-neutron shell-gap energies around $N=50$ with theoretical predictions, we have shown that HFB-24 and DZ10 represent the two extremes of the studied mass models, and were therefore selected for systematic studies of the electron-capture rates during the core collapse of a massive star. The corresponding difference in the instantaneous electron-capture rates between the HFB-24 and DZ10 models, was investigated with a fixed and a self-consistent core-collapse supernova trajectory. We have shown that there is a strong feedback effect between the hydrodynamics and the microphysics, namely the equation of state and electron-capture rates, thus highlighting the need to perform numerical simulations to have a more realistic and quantitative evaluation of the impact of nuclear-physics data on astrophysical predictions. More details concerning the data analysis (e.g. identification and characterization of ground states and isomeric states when relevant) and the CCSN simulations results will be given in a forthcoming paper. Lastly, our new mass-excess values will allow better electron-capture Q-value calculations of key nuclei for CCSN (see the inset of Fig. 3). Although the electron-capture rates for these key nuclei should be experimentally constrained to have a full control of the core collapse modeling [55], the Q-values are a basic ingredient in the rate calculation, meaning that our results constitute a first important step in this direction.

Declaration of competing interest

The authors declare that they have no known competing financial interests or personal relationships that could have appeared to influence the work reported in this paper.

Data availability

Data will be made available on request.

Acknowledgements

This work has been supported by the Academy of Finland Grant No. 284612 (the Finnish Centre of Excellence Program in Nuclear and Accelerator Based Physics Research at JYFL 2012-2017) and by the European Union's Horizon 2020 Research and Innovation Programme Grant Agreement No. 654002 (ENSAR2). A.K. acknowledges support from the Academy of Finland under Grant No. 275389, and D.A.N. and L.C. acknowledge support under Grants No. 284516 and No. 312544. T.E. acknowledges support from the Academy of Finland under Grant No. 295207, and A.d.R. acknowledges support under Grant No. 306980. A.K. and L.C. acknowledge the funding from the European Union's Horizon 2020 Research and Innovation Programme under Grant Agreement No. 771036 (ERC CoG MAIDEN). We are grateful for the bilateral mobility Grants from the Institut Français in Finland, the Embassy of France in Finland, the French Ministry of Higher Education and Research, and the Finnish Society of Science and Letters. We are grateful for the mobility support from Projet International de Coopération Scientifique Manipulation of Ions in Traps and Ion sourCes for Atomic and Nuclear Spectroscopy (MITICANS). S.G. is grateful for the mobility Grant from the EDPSIME. S.G. was supported by NSF Grants No. PHY-1913554 (Windows on the Universe: Nuclear Astrophysics at the NSCL). Partial support from the CNRS PICS07889 is acknowledged. We would like to thank J. Pons for providing us with the original version of the ACCEPT code.

References

[1] P. Cerda-Duran, N. Elias-Rosa, Neutron Stars Formation and Core Collapse Supernovae, Springer International Publishing, Cham, 2018, pp. 1–56.
[2] H.-T. Janka, K. Langanke, A. Marek, G. Martínez-Pinedo, B. Müller, Theory of core-collapse supernovae, in: The Hans Bethe Centennial Volume 1906-2006, Phys. Rep. 442 (1) (2007) 38–74, https://doi.org/10.1016/j.physrep.2007.02.002.
[3] A. Burrows, Colloquium: perspectives on core-collapse supernova theory, Rev. Mod. Phys. 85 (2013) 245–261, https://doi.org/10.1103/RevModPhys.85.245.
[4] A. Pascal, S. Giraud, A.F. Fantina, F. Gulminelli, J. Novak, et al., Impact of electron capture rates for nuclei far from stability on core-collapse supernovae, Phys. Rev. C 101 (2020) 015803, https://doi.org/10.1103/PhysRevC.101.015803.
[5] A.R. Raduta, F. Gulminelli, M. Oertel, Modification of magicity toward the dripline and its impact on electron-capture rates for stellar core collapse, Phys. Rev. C 93 (2016) 025803, https://doi.org/10.1103/PhysRevC.93.025803.
[6] S. Furusawa, H. Nagakura, K. Sumiyoshi, C. Kato, S. Yamada, Dependence of weak interaction rates on the nuclear composition during stellar core collapse, Phys. Rev. C 95 (2017) 025809, https://doi.org/10.1103/PhysRevC.95.025809.
[7] C. Sullivan, E. O'Connor, R.G.T. Zegers, T. Grubb, S.M. Austin, The sensitivity of core-collapse supernovae to nuclear electron capture, Astrophys. J. 816 (1) (2015) 44, https://doi.org/10.3847/0004-637x/816/1/44.
[8] G. Grams, S. Giraud, A.F. Fantina, F. Gulminelli, Distribution of nuclei in equilibrium stellar matter from the free-energy density in a Wigner-Seitz cell, Phys. Rev. C 97 (2018) 035807, https://doi.org/10.1103/PhysRevC.97.035807.
[9] M. Arnould, S. Goriely, K. Takahashi, The r-process of stellar nucleosynthesis: astrophysics and nuclear physics achievements and mysteries, Phys. Rep. 450 (4) (2007) 97–213, https://doi.org/10.1016/j.physrep.2007.06.002.
[10] M. Mumpower, R. Surman, G. McLaughlin, A. Aprahamian, The impact of individual nuclear properties on r-process nucleosynthesis, Prog. Part. Nucl. Phys. 86 (2016) 86–126, https://doi.org/10.1016/j.ppnp.2015.09.001.
[11] C.J. Horowitz, A. Arcones, B. Côté, I. Dillmann, W. Nazarewicz, et al., r-process nucleosynthesis: connecting rare-isotope beam facilities with the cosmos, J. Phys. G, Nucl. Part. Phys. 46 (8) (2019) 083001, https://doi.org/10.1088/1361-6471/ab0849.
[12] S. Brett, I. Bentley, N. Paul, R. Surman, A. Aprahamian, Sensitivity of the r-process to nuclear masses, Eur. Phys. J. A 48 (12) (2012) 184, https://doi.org/10.1140/epja/i2012-12184-4.
[13] A. Aprahamian, I. Bentley, M. Mumpower, R. Surman, Sensitivity studies for the main r process: nuclear masses, AIP Adv. 4 (4) (2014) 041101, https://doi.org/10.1063/1.4867193.
[14] M.P. Reiter, S.A. San Andrés, S. Nikas, J. Lippuner, C. Andreoiu, et al., Mass measurements of neutron-rich gallium isotopes refine production of nuclei of the first r-process abundance peak in neutron-star merger calculations, Phys. Rev. C 101 (2020) 025803, https://doi.org/10.1103/PhysRevC.101.025803.
[15] J. Bliss, A. Arcones, F. Montes, J. Pereira, Nuclear physics uncertainties in neutrino-driven, neutron-rich supernova ejecta, Phys. Rev. C 101 (2020) 055807, https://doi.org/10.1103/PhysRevC.101.055807.
[16] P.T. Hosmer, H. Schatz, A. Aprahamian, O. Arndt, R.R.C. Clement, et al., Half-life of the doubly magic r-process nucleus ^{78}Ni, Phys. Rev. Lett. 94 (2005) 112501, https://doi.org/10.1103/PhysRevLett.94.112501.
[17] Z.Y. Xu, S. Nishimura, G. Lorusso, F. Browne, P. Doornenbal, et al., β-decay half-lives of ^{76,77}Co, ^{79,80}Ni, and ^{81}Cu: experimental indication of a doubly magic ^{78}Ni, Phys. Rev. Lett. 113 (2014) 032505, https://doi.org/10.1103/PhysRevLett.113.032505.
[18] A. Welker, N.A.S. Althubiti, D. Atanasov, K. Blaum, T.E. Cocolios, et al., Binding energy of ^{79}Cu: probing the structure of the doubly magic ^{78}Ni from only one proton away, Phys. Rev. Lett. 119 (2017) 192502, https://doi.org/10.1103/PhysRevLett.119.192502.
[19] R. Taniuchi, C. Santamaria, P. Doornenbal, A. Obertelli, K. Yoneda, et al., ^{78}Ni revealed as a doubly magic stronghold against nuclear deformation, Nature 569 (7754) (2019) 53–58, https://doi.org/10.1038/s41586-019-1155-x.
[20] S. Rahaman, J. Hakala, V.-V. Elomaa, T. Eronen, U. Hager, et al., Masses of neutron-rich Ni and Cu isotopes and the shell closure at Z= 28, N= 40, Eur. Phys. J. A 34 (1) (2007) 5–9.
[21] I. Moore, T. Eronen, D. Gorelov, J. Hakala, A. Jokinen, et al., Towards commissioning the new IGISOL-4 facility, in: XVIth International Conference on ElectroMagnetic Isotope Separators and Techniques Related to Their Applications, December 2–7, 2012 at Matsue, Japan, Nucl. Instrum. Methods Phys. Res., Sect. B 317 (2013) 208–213, https://doi.org/10.1016/j.nimb.2013.06.036.
[22] P. Karvonen, I. Moore, T. Sonoda, T. Kessler, H. Penttilä, et al., A sextupole ion beam guide to improve the efficiency and beam quality at IGISOL, Nucl. Instrum. Methods Phys. Res., Sect. B 266 (21) (2008) 4794–4807, https://doi.org/10.1016/j.nimb.2008.07.022.
[23] A. Nieminen, J. Huikari, A. Jokinen, J. Äystö, P. Campbell, et al., Beam cooler for low-energy radioactive ions, Nucl. Instrum. Methods Phys. Res., Sect. A 469 (2) (2001) 244–253, https://doi.org/10.1016/S0168-9002(00)00750-6.
[24] T. Eronen, V.S. Kolhinen, V.V. Elomaa, D. Gorelov, U. Hager, et al., JYFLTRAP: a Penning trap for precision mass spectroscopy and isobaric purification, Eur. Phys. J. A 48 (4) (2012) 46, https://doi.org/10.1140/epja/i2012-12046-1.
[25] G. Savard, S. Becker, G. Bollen, H.-J. Kluge, R. Moore, et al., A new cooling technique for heavy ions in a Penning trap, Phys. Lett. A 158 (5) (1991) 247–252, https://doi.org/10.1016/0375-9601(91)91008-2.
[26] M. König, G. Bollen, H.J. Kluge, T. Otto, J. Szerypo, Quadrupole excitation of stored ion motion at the true cyclotron frequency, Int. J. Mass Spectrom. Ion Process. 142 (1–2) (1995) 95–116, https://doi.org/10.1016/0168-1176(95)04146-C.
[27] M. Kretzschmar, The Ramsey method in high-precision mass spectrometry with Penning traps: theoretical foundations, Int. J. Mass Spectrom. 264 (2) (2007) 122–145, https://doi.org/10.1016/j.ijms.2007.04.002.
[28] S. George, S. Baruah, B. Blank, K. Blaum, M. Breitenfeldt, et al., Ramsey method of separated oscillatory fields for high-precision Penning trap mass spectrometry, Phys. Rev. Lett. 98 (2007) 162501, https://doi.org/10.1103/PhysRevLett.98.162501.
[29] M. Wang, W. Huang, F. Kondev, G. Audi, S. Naimi, The AME 2020 atomic mass evaluation (II). Tables, graphs and references, Chin. Phys. C 45 (3) (2021) 030003, https://doi.org/10.1088/1674-1137/abddaf.
[30] L. Canete, A. Kankainen, T. Eronen, D. Gorelov, J. Hakala, et al., High-precision mass measurements of ^{25}Al and ^{30}P at JYFLTRAP, Eur. Phys. J. A 52 (5) (2016) 124, https://doi.org/10.1140/epja/i2016-16124-0.
[31] L. Canete, High precision mass measurements for nuclear astrophysics, Ph.D. thesis, University of Jyväskylä, 2019, https://jyx.jyu.fi/handle/123456789/62968.
[32] A. Estradé, M. Matoš, H. Schatz, A.M. Amthor, D. Bazin, et al., Time-of-flight mass measurements for nuclear processes in neutron star crusts, Phys. Rev. Lett. 107 (2011) 172503, https://doi.org/10.1103/PhysRevLett.107.172503.
[33] J. Stadlmann, M. Hausmann, F. Attallah, K. Beckert, P. Beller, et al., Direct mass measurement of bare short-lived ^{44}V, ^{48}Mn, ^{41}Ti and ^{45}Cr ions with isochronous mass spectrometry, Phys. Lett. B 586 (1) (2004) 27–33, https://doi.org/10.1016/j.physletb.2004.02.014.
[34] Y. Xing, K. Li, Y. Zhang, X. Zhou, M. Wang, et al., Mass measurements of neutron-deficient Y, Zr, and Nb isotopes and their impact on rp and νp nucleosynthesis processes, Phys. Lett. B 781 (2018) 358–363, https://doi.org/10.1016/j.physletb.2018.04.009.
[35] W.R. Plaß, T. Dickel, U. Czok, H. Geissel, M. Petrick, et al., Isobar separation by time-of-flight mass spectrometry for low-energy radioactive ion beam fa-

cilities, in: Proceedings of the XVth International Conference on Electromagnetic Isotope Separators and Techniques Related to Their Applications, Nucl. Instrum. Methods Phys. Res., Sect. B 266 (19) (2008) 4560–4564, https://doi.org/10.1016/j.nimb.2008.05.079.

[36] I. Mardor, S.A. San Andrés, T. Dickel, D. Amanbayev, S. Beck, et al., Mass measurements of As, Se, and Br nuclei, and their implication on the proton-neutron interaction strength toward the $N = Z$ line, Phys. Rev. C 103 (2021) 034319, https://doi.org/10.1103/PhysRevC.103.034319.

[37] M. Matoš, A. Estrade, M. Amthor, A. Aprahamian, D. Bazin, et al., TOF-bρ mass measurements of very exotic nuclides for astrophysical calculations at the NSCL, J. Phys. G, Nucl. Part. Phys. 35 (1) (2007) 014045, https://doi.org/10.1088/0954-3899/35/1/014045.

[38] M. Zach, Mapping the frontiers of the nuclear mass surface, J. Phys. Conf. Ser. 1668 (2020) 012026, https://doi.org/10.1088/1742-6596/1668/1/012026.

[39] D.A. Nesterenko, T. Eronen, A. Kankainen, L. Canete, A. Jokinen, et al., Phase-Imaging Ion-Cyclotron-Resonance technique at the JYFLTRAP double Penning trap mass spectrometer, Eur. Phys. J. A 54 (9) (2018) 154, https://doi.org/10.1140/epja/i2018-12589-y.

[40] C. Guénaut, G. Audi, D. Beck, K. Blaum, G. Bollen, et al., High-precision mass measurements of nickel, copper, and gallium isotopes and the purported shell closure at $N = 40$, Phys. Rev. C 75 (2007) 044303, https://doi.org/10.1103/PhysRevC.75.044303.

[41] S. Baruah, G. Audi, K. Blaum, M. Dworschak, S. George, et al., Mass measurements beyond the major r-process waiting point ^{80}Zn, Phys. Rev. Lett. 101 (2008) 262501, https://doi.org/10.1103/PhysRevLett.101.262501.

[42] J. Hakala, S. Rahaman, V.-V. Elomaa, T. Eronen, U. Hager, et al., Evolution of the $N = 50$ shell gap energy towards ^{78}Ni, Phys. Rev. Lett. 101 (2008) 052502, https://doi.org/10.1103/PhysRevLett.101.052502.

[43] L. Canete, S. Giraud, A. Kankainen, B. Bastin, F. Nowacki, et al., Precision mass measurements of ^{67}Fe and ^{69,70}Co: nuclear structure toward $N = 40$ and impact on r-process reaction rates, Phys. Rev. C 101 (2020) 041304, https://doi.org/10.1103/PhysRevC.101.041304.

[44] J.M. Pearson, N. Chamel, A.Y. Potekhin, A.F. Fantina, C. Ducoin, et al., Unified equations of state for cold non-accreting neutron stars with Brussels–Montreal functionals – I. Role of symmetry energy, Mon. Not. R. Astron. Soc. 481 (3) (2018) 2994–3026, https://doi.org/10.1093/mnras/sty2413.

[45] J. Duflo, A. Zuker, Microscopic mass formulas, Phys. Rev. C 52 (1995) R23–R27, https://doi.org/10.1103/PhysRevC.52.R23.

[46] P. Möller, A. Sierk, T. Ichikawa, H. Sagawa, Nuclear ground-state masses and deformations: Frdm(2012), At. Data Nucl. 109–110 (2016) 1–204, https://doi.org/10.1016/j.adt.2015.10.002.

[47] S. Goriely, N. Chamel, J.M. Pearson, Further explorations of Skyrme-Hartree-Fock-Bogoliubov mass formulas. XIII. The 2012 atomic mass evaluation and the symmetry coefficient, Phys. Rev. C 88 (2013) 024308, https://doi.org/10.1103/PhysRevC.88.024308.

[48] N. Wang, M. Liu, X. Wu, J. Meng, Surface diffuseness correction in global mass formula, Phys. Lett. B 734 (2014) 215–219, https://doi.org/10.1016/j.physletb.2014.05.049.

[49] H. Koura, T. Tachibana, M. Uno, M. Yamada, Nuclidic mass formula on a spherical basis with an improved even-odd term, Prog. Theor. Phys. 113 (2) (2005) 305–325, https://doi.org/10.1143/PTP.113.305.

[50] J.V. Romero, J.M.A. Ibanez, J.M.A. Marti, J.A. Miralles, A new spherically symmetric general relativistic hydrodynamical code, Astrophys. J. 462 (1996) 839, https://doi.org/10.1086/177198.

[51] J.V. Romero, J.M. Miralles, J.A. Ibáñez, J.A. Pons, General relativistic collapse of hot stellar cores, in: J.A. Miralles, J.A. Morales, D. Saez (Eds.), Some Topics on General Relativity and Gravitational Radiation, 1997, p. 289.

[52] A.F. Fantina, Supernovae theory: study of electro-weak processes during gravitational collapse of massive stars, Ph.D. thesis, Université Paris Sud - Paris XI, 2010, https://tel.archives-ouvertes.fr/tel-00566480.

[53] J.M. Lattimer, D.F. Swesty, A generalized equation of state for hot, dense matter, Nucl. Phys. A 535 (2) (1991) 331–376, https://doi.org/10.1016/0375-9474(91)90452-C.

[54] K. Langanke, G. Martínez-Pinedo, J.M. Sampaio, D.J. Dean, W.R. Hix, et al., Electron capture rates on nuclei and implications for stellar core collapse, Phys. Rev. Lett. 90 (2003) 241102, https://doi.org/10.1103/PhysRevLett.90.241102.

[55] K. Langanke, G. Martínez-Pinedo, R.G.T. Zegers, Electron capture in stars, Rep. Prog. Phys. 84 (6) (2021) 066301, https://doi.org/10.1088/1361-6633/abf207.